Proceedings 8th Symposium on
Meteorological Observations and Instrumentation,
17-22 January 1993, Anaheim, California

15.3

MEASUREMENTS ON CONTRAILS OF COMMERCIAL AIRCRAFT

Robert Baumann, Reinhold Busen, Hans P. Fimpel,
Christoph Kiemle, Manfred E. Reinhardt

DLR, Institute of Atmospheric Physics
D-8031 Oberpfaffenhofen, Germany

Markus Quante

GKSS Research Center, Institute for Physics
2054 Geesthacht, Germany

1. INTRODUCTION

The rapid increase in subsonic air traffic and the public concern on environmental damages has initiated in Germany a program on "Air Traffic and the Environment", which consist of different projects by DLR, other research institutes, and the industry.

The measurements on contrails of commercial aircraft are part of this program. The main goals are to investigate the spatial extent, the structure, the dynamics, and the life cycle of contrails under different meteorological conditions, to look after the turbulent properties inside and outside the contrails, to explain the reasons for fast dilution or very far broadening of contrails, and to measure the chemical composition of the exhaust.

There has been some work on some of these questions in the past, but mainly focussed on supersonic aircraft (e.g. CIAP, 1975; Miake-Lye et al., 1992). Especially there are no insitu measurements at cruising speed and altitude up to now.

This paper gives a description of methods for investigations on contrails, which have been applied using the DLR Falcon jet, together with some first results.

2. STRATEGY OF MEASUREMENTS AND INSTRUMENTATION

There are two different modes for inspecting contrails, they are outlined in Figure 1. Contrails can be investigated from outside by applying remote sensing techniques. For this purpose a LIDAR system installed on the Falcon is used. On the other hand, by flying inside and close to the contrail, the meteorological and chemical properties of the contrail itself and its immediate surrounding can be measured. This leads to chemical compositions, spectra of the turbulent energy, and geometrical dimensions at different distances of the leading airliner. Those methods are described in the next paragraphs.

The measurements itself and also the data evaluation are made more difficult by the fact, that steadily flying inside a contrail is an unpossible thing to do. As the Falcon is small and light compared to the commercial aircraft to be followed, it is heavily exposed to the turbulence and the vortices, which results in getting thrown there and back inside and also out of the contrail. This causes a lot of variances e.g. in the data describing the aircraft attitude, which carefully have to be considered during the data evaluation.

The helpful support of the air traffic control authority did also play an important role in our strategy of measurements. Under guidance of a controller the Falcon first was lead to a course parallel to that of the airliner of interest and at a flight level some hundreds of meters above. As the Falcon was normally slightly slower than an airliner, the Falcon first flew ahead of the airliner and then descended after the aircraft below had overtaken. In case of the remote measurements, the Falcon stayed at the higher flight level as the LIDAR-System is looking downwards.

For the recording of the distance between the both aircrafts and the airspeed and height of the airliner as a function of time, we filmed the radar screen at the air traffic control center with a video camera. On board of the Falcon also two video cameras were installed, one looking forward through the front window, and one looking downwards through the same window as the LIDAR-System.

An Inertial Reference System (IRS) allows the precise measurement of the Falcon's attitude angles, components of the velocity vector and three-dimensional position.

2.1 Remote Sensing of Contrails

Within the DLR Institute of Atmospheric Physics an airborne near infrared Differential Absorption Lidar (DIAL) is operated for meteorological applications. This system is based on a Nd:YAG pumped narrow band tunable dye laser for both on- and off-line measurements. Two dimensional distributions of water vapor, range resolved horizontal and vertical water vapor profiles, horizontal power spectra of turbulence, and aerosol backscattering profiles are the result (Ehret et al., 1992).

The latter are used for the investigation of contrail shape and size. The aerosol backscatter signal provided by the Lidar system is sampled at a rate of 10 MHz with a resolution of 12 bits, leading to a high aerosol density resolution. The vertical resolution amounts to 15 m, whereas the horizontal resolution depends on the laser shot repetition rate and the true air speed of the aircraft. Typical speeds are

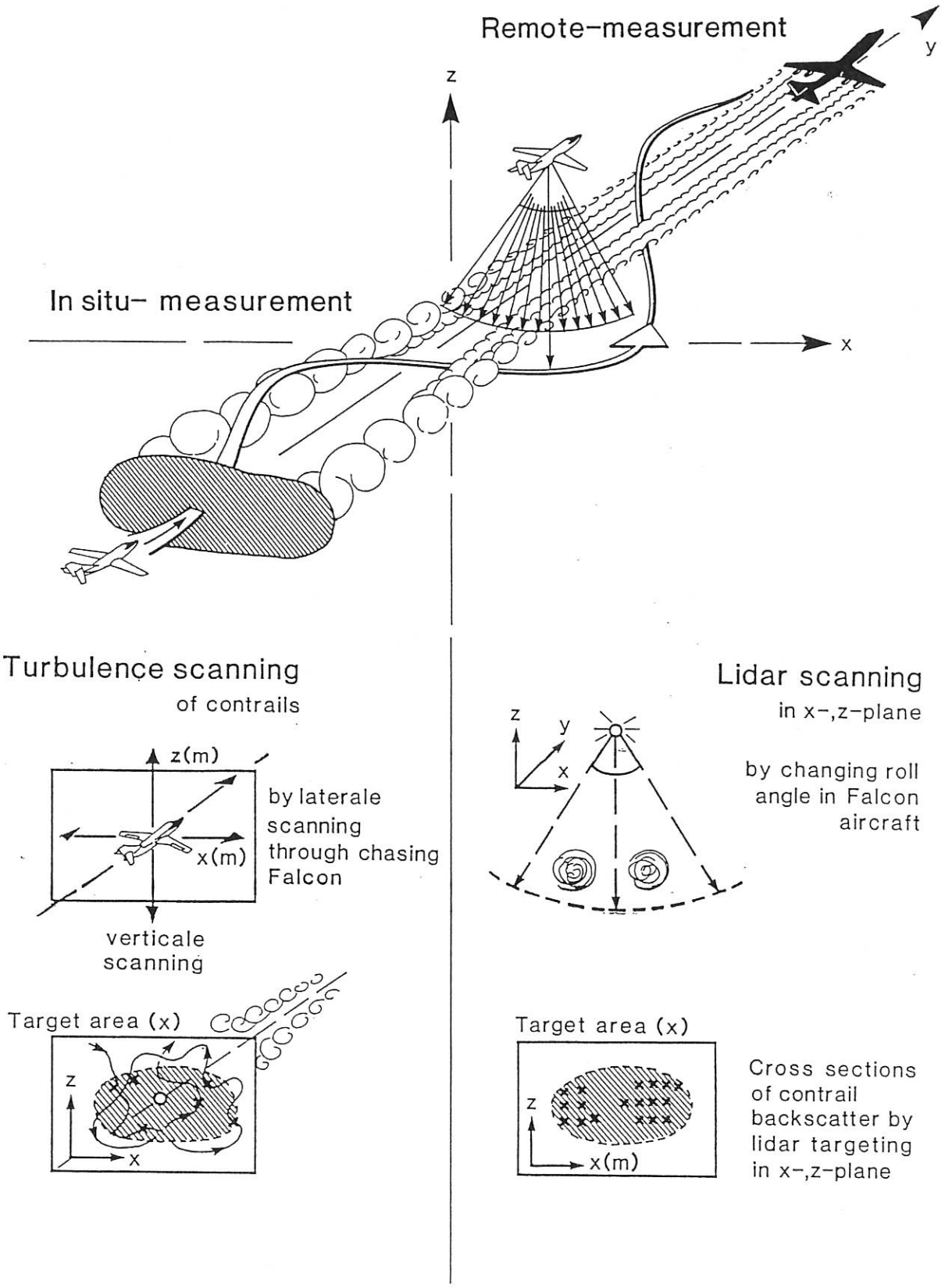

Figure 1. Illustration of the measurement strategy.

about 200 m/s, and with a repetition rate of nearly 10 Hz the horizontal resolution is about 20 m.

As the minimal vertical distance between the Falcon an the airliner below is around 600 m (optimal working of the LIDAR-System), it is rather difficult for the pilot, to fly exactly above and along the contrail, especially in cases of poor optical contrast against lower lying clouds. So we used two methods of scanning over a contrail. The first one is through slowly horizontal yawing left and right, resulting in a flight path which is slightly wavy with deviations from a straight line in the order of some tens of meters. By this, the laser beam crosses the contrail twice each period of the yaw-movement under a small angle. The second scan method is by applying periodical roll maneuvers resulting in a movement of the laser beam similar to a pendulum swinging across the contrail.

2.2 Dimension of Contrails from In-Situ Measurements

For the in-situ measurements the Falcon is instrumented with fast response pressure transducers, an open-wire platinum resistance thermometer, a fast Lyman-α hygrometer and a 5-hole flow angle sensor for measuring true airspeed and angles of attack and sideslip, mounted on the tip of a 1.8 m nose boom. Their data were sampled and recorded at a rate of 100 Hz, after passing analogue filters with a cut-off frequency of 50 Hz. The three components of wind vector were calculated using the data of the IRS and the velocity of the aircraft with respect to the air as obtained from data of the flow angle sensor (e.g. Bögel, 1991; Lenschow, 1984).

To get information about geometrical dimensions and profiles of thermodynamic properties across the axis, we tried to scan vertically and horizontally through the axis of the contrail at different distances to the aircraft flying ahead of the Falcon.

2.3 Turbulence Spectra from In-Situ Measurements

To investigate statistical properties of the turbulence we tried to fly in the center or at the boundary zone as long as possible (up to 50 seconds). Due to the heavy turbulences and the strong vortices, this is hard to fly and often the Falcon was suddenly thrown out of the contrail.

The total time in or close to the contrail of a certain aircraft was up to 5 minutes, depending on the difference of the speed between the airliner and the Falcon.

3. RESULTS OF MEASUREMENTS

3.1 Vertical Descending, Geometry and Aerosol Profiles

Figure 2 shows indirectly the measured height of the contrail of a Boing 747-200 as a function of the distance to the producing aircraft: the x-axis showing the time of measurement, t, is nearly linearly correlated with the distance variing from 4.2 km on the left side to 15.4 km on the right side, as the Falcon flew between 30 and 40 m/s slower than the Boing 747-200 below. The distances were measured from the video recordings of the radar screen within an accuracy of about 0.5 km. The y-axis of the figure shows the following value:

$$h_p - r^{(i)} \cos \Phi \qquad (1)$$

where h_p is the (pressure) altitude of the Falcon, $r^{(i)}$ is the distance corresponding to the i-th datapoint (or window of transit time) of the aerosol-backscatter signal of a single laser shot, which is, at a sampling rate of 10 MHz, i times 15 m, and Φ is the roll angle of the Falcon. The thickness of each of the lines, corresponding to one specific value of i, is modulated by the factor $f_n S_a^{(i)}(t)$, where $S_a^{(i)}(t)$ is the value of the aerosol signal at the i-th time window of the laser shot at the time t and f_n an arbitrary normalizing factor.

By this, areas with thick 'lines' (or peaks on the lines) correspond to areas with high backscatter signal indicating the height of the contrail as a function of distance (the laser beam only occasionally hit the contrail, as the Falcon was scanning horizontally across the contrail as described in section 2.1). From the figure it can be seen, that the contrail descended about 120 m over the shown range of distances, i.e. about 1.1 % of the distance variation, or in terms of a velocity, with about 2.5 m/s. The B 747-200 flew at about 10670 m height with a true airspeed of 225 m/s, the Falcon around 1200 m higher with variations of up to 100 m resulting from the scanning maneuvers.

To investigate the geometry and aerosol profiles across the contrail, we needed to evaluate the flight path of the Falcon with a relative accuracy in the order of a few meters. More exact, we had to evaluate the path of the point of intersection of the laser beam with a plane in the height of the measured contrail. By marking those sections of the path, from where a certain backscatter signal was detected, and connecting these pieces with one or two straight lines, according to the number of visible strips of the contrail, we got the information about the main direction of the contrail. This was used to rotate the axes of the coordinate frame such, that one axis looks along the average track of the contrail and the other one across.

With x, the east-west component of the relative position (positive to the east), and y, the north-south component (positive to the north), the transformed coordinates become

$$\begin{aligned} x' &= x \cos \Psi - y \sin \Psi \\ y' &= x \sin \Psi + y \cos \Psi \end{aligned} \qquad (2)$$

where Ψ is the angle by which the frame has been rotated clockwise. In this frame, x' is the cross-track distance of the Falcon with respect to the contrail's track, when Ψ is set to the main direction of the contrail (counted clockwise from north), and the origin is shifted to somewhere within the contrail. x and y are calculated by integration of the east-west component, u_K, and the north-south component, v_K of the Falcon's groundspeed, measured by the IRS.

$$x(t) = \int_{t_0}^{t} u_K(\tau)\, d\tau \qquad y(t) = \int_{t_0}^{t} v_K(\tau)\, d\tau \qquad (3)$$

The cross-track distance x'_L of the above mentioned point of intersection of the laser beam with a plane in the height h_L is given by

$$x'_L = x' - (h_p - h_L) \tan \Phi \qquad (4)$$

where Φ is the roll angle and h_p the altitude of the Falcon. x'_L is also the horizontal distance to the contrail plus a constant offset as long as the producing aircraft is flying with constant course and the contrail is not wavy due to wind shear or its own dynamic. In the case shown below this seems to be a good assumption up to 7 km behind the airliner.

Figure 3 shows a plot of the section between 4.2 km and 7.4 km behind the B 747-200. The scanning was some kind of combination of yawing and gentle rolling. The upper

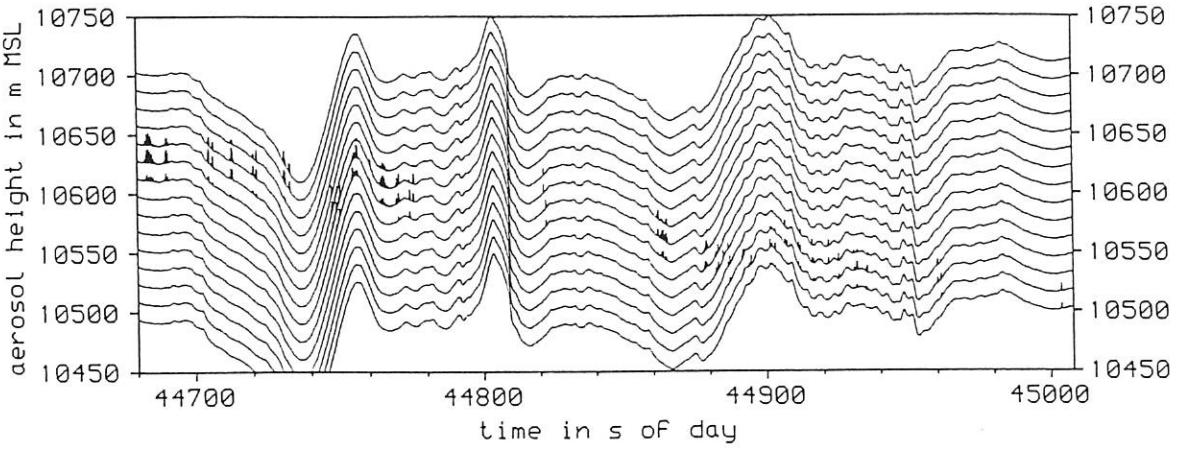

Figure 2. Height of a contrail as a function of increasing distance from the producing B 747-200 aircraft from LIDAR measurements. The distance varies nearly linear from 4.2 km on the left margin to 15.4 km on the right margin. The lines represent the height, out of which the backscatter signal comes, that has been measured within a certain window of transit time, as it results from the Falcon's altitude and roll angle. Thicker lines or peaks on the lines reflect higher backscatter signal and mark the position of hitted parts of the contrail.

part shows the averaged aerosol-backscatter signal from an altitude range that covers the vertical extent of the contrail, over the time of measurement, t. The medium part shows the cross-track distance of the Falcon, x' (long-dashed line), and of the beam intersection with a plane at 10615 m, x'_L (short-dashed line). The graph can be interpreted similar to a 2-dimensional projection of the track from above to a map with extreme different scales for the two axes. The time segment of 100 s corresponds to a along-track distance, y', of 17 km. Those parts of the track corresponding to an aerosol signal of more than 25 % of the highest peaks are marked with thicker full lines. The lower part shows the roll angle Φ to illustrate the main source of the large amplitudes in x'_L (c.f. (4) on page 7).

As can be seen, the hits of the first four crossings (i.e. between t=44685 s and 44732 s) lie on two strips of around 13 to 20 m width each. The distance between the centers is around 40 to 48 m, the variation in the position of the center in the order of 5 m (note that the absolute values of x' and x'_L are shifted due to an arbitrary definition of the origin of the x'-y'-frame which does not influence the relative values). In the right part of the plot the contrail bends rightwards, which could result from slight corrections in the course of the airliner in the order of 0.3° or from variations in the windfield. Beyond a distance of 7 km from the B 747-200 ahead the structure of this contrail has become wavy with the two strips mostly swinging in counterphase, as could also be seen on the video looking downwards.

The scanning speed, i.e. the time derivation of x'_L, was in the range of 5 to 40 m/s. In a coordinate frame moving with the wind this corresponds to a crossing angle of 1.5° to 12°, in a coordinate frame moving with the speed of the producing aircraft, the crossing angle was in the range from 10° to 50°.

Figure 4 shows a profile of the aerosol signal of one single scan across the contrail of the B 747-200, i.e. the backscatter signal over the cross-track distance x'_L. Each of the sqares represents the data of one single laser shot, reflecting the total aerosol amount (in arbitrary units) within a thin vertical cylinder covering the vertical extent of the

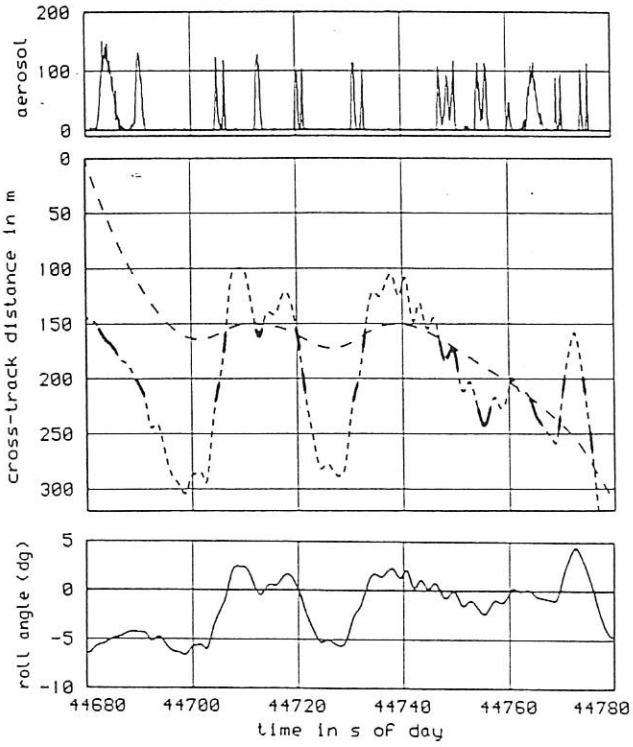

Figure 3. LIDAR measurement of horizontal geometry of the contrail of a B 747-200. Top: aerosol backscatter signal during horizontal scanning as a function of time. Mid: cross-track distance to the reference track of the Falcon (x', long-dashed line), and of the intersection of the laser beam with a plane at a height of 10615 m (x'_L, short-dashed line). Hits of the contrail (see graph on top of figure) are marked with full lines. Further explanation see text. Bottom: roll angle during scan.

contrail at the shown x'_L, sampled along the track through the contrail as shown in Figure 3 above (t=44680 s - 44693 s). The distance between the center of the two stripes is 43 m and the 50%-width 15 m and 12 m respectively.

The example is taken from a rather slow scan ($\dot{x}'_L = 5 - 10$m/s) through the contrail with small crossing angle at a mean distance of 4.4 km. The profile therefore results from a superposition of the cross-section profile at the mean distance and some unknown longitudinal modulation of density and cross-section. Some part or all of the unsymmetry in the profiles of the two stripes might be due to this latter difficulty. In the shown example the crossing took 4.3 s for the left stripe and 1.8 s for the right stripe. Therefore the crossing was along a length of 750 and 300 m respectively. On the other hand, increasing of the scan speed reduces the influence of longitudinal structures on the measurement of cross-sections indeed, but it also reduces the number of laser shots hitting the contrail, reducing the spatial resolution, so there is always some compromise to be made. For example, by using periodical roll maneuvers with roll angles of ± 5 ° and a period of 10 s, the scan speed reaches more than 60 m/s at a height of 1200 m below of the Falcon, resulting in only two or three 'hits' of a stripe per passage.

3.2 In-Situ Measurements of Cross-Sections

For that cases of measurements inside of a contrail, which we analyzed up to now, the evaluation of a position with respect to the contrail suffers from the fact, that the contrails seemed not to have such a clear and simple structure as e.g. in the case of the remote measurements of the B 747-200 shown above. At the remote measurements we had an additional information from the video recordings of the camera looking downwards. During the in-situ measurements however, the recordings of the camera looking forward is much more difficult to interpret, as the density of the visible contrail was very low in most cases.

Though the evaluation of the Falcon's track seems to be possible within a relative accuracy of a few meters for time scales of some minutes, as could be seen e.g. from Fig. 3, there is no direct information about the position of the contrail. Even if the airliner would move through the space along an idealized straight line, the contrail might be wavy due to its own dynamic or wind sheer. So the form and structure of a contrail can only be reconstructed by using some assumptions, the Falcons' flight track and the measurements of temperature, humidity and wind components.

In contrast to the Lidar measurements, where the aerosol signal of each laser shot can be integrated over the whole vertical extent of the contrail, the in-situ-measurements can only provide data along a relatively complicated and arbitrary path through or nearby the contrail. So the two-dimensional projection of the flight path as in Fig. 3, marked with some suitable indicator for inside of the contrail, has to be interpreted very carefully in addition with the altitude of the track and is only possible, when the contrail has little deviations from a straight line compared to it's width. At the moment we are searching for some suitable cases, but the presentation of the present state of evaluation would exceed the scope of this abstract.

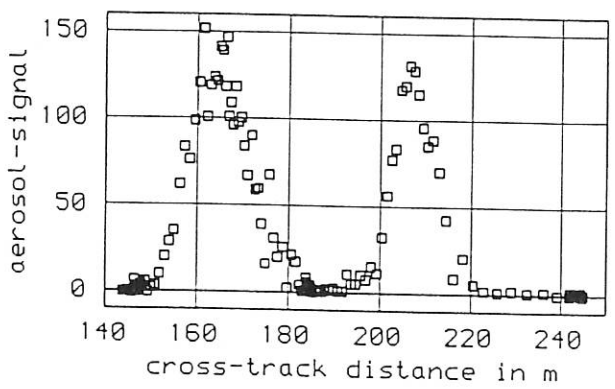

Figure 4. Profile of aerosol concentration of the contrail of a B 747-200. The cross-track distance represents the relative distance to the axis of the contrail plus an arbitrary offset.

3.3 Turbulence Spectra

In order to examine the dynamical structure of a contrail, power spectra of the three wind components , u, v, and w, have been analysed. Since time slots the Falcon has spent inside the contrail at an approximate constant distance behind the leading aircraft were relatively short (typical time segments vary between 10 and 40 sec.), conventional spectral analysis via FFT was not feasible. We calculated the spectra applying the maximum entropy method (MEM), first proposed by Burg (1967). MEM has the advantage of being able to find sharp spectral peaks which the Fourier methods fail to resolve. MEM spectra show also considerable promise when the length of the time series is limited (Haykin, 1983), which is often the case in instationary flows. For red noise processes the MEM shows in this case superior results compared to conventional methods (Fougere, 1985).

The principle idea of the MEM is to calculate that spectrum which corresponds to the most random or most unpredictable time series whose autocorrelation function agrees with the known values. Assumptions like periodic extension of the data outside the available record length are avoided. The problem with the MEM is, that at present there is no objective criterion for choosing the optimal number of filter coefficients, the order of the process. Too many coefficients can result in spurious spectral features. On the other hand the number of coefficients must be high enough to resolve narrow peaks in the spectrum. In practice the spectra were calculated for different filter orders and conclusions are made on the basis of several estimated spectra.

The applied algorithm is based on the autoregressive representation of the time series and has been developed with the intention to minimise the so called 'line-splitting' effect. It is described by Barrodale and Erickson (1980).

In this manner power spectra for u, v, and w have been estimated for samples gathered inside the contrail and for reference segments in undisturbed air. In Fig. 5 an example time series for w inside the contrail is shown. The Falcon flew about 2 km behind the leading aircraft, a DC-9. Typical fluctuations of w are on the order of 1 m/s.

Different spectra for the three velocity components for several in-contrail samples at a fixed distance behind the producing aircraft show basically the same behaviour. Compared to spectra for data gathered in undisturbed air a great deal of structure is abvious. Isolated peaks point to to the existence of dominate eddies (coherent structures).

Assuming Taylor's hypothesis on the basis of the true airspeed, frequency can be converted to wavelength. Characteristic wavelengths for spectral peaks vary between 70 m and 200 m. It has to be mentioned that the interpretation of the single spectral peaks has to consider the variable position of the Falcon within the contrail. Ensembles of coherent structures could be sampled at different distances with respect to their centerlines. An example of w-spectra for time segments inside and outside the contrail is presented in Fig. 6. The underlying time series for the in-contrail case is that shown in Fig. 5, the length of the flight segment was about 10 km. The spectral amplitude inside the contrail is 1 to 2 orders of magnitude higher compared to the clear air case, indicating a considerable dynamical activity. A developed energy cascade is not present, while the spectrum for the undisturbed case rolls of with a slope of about -5/3.

A broader spectral peak occurs in all w-spectra in the frequency range of about 5 to 20 Hz, corresponding to a wavelength interval of 45 m to 12 m with a maximum around 18 m, which should be the size of the smallest dominant eddies.

In further evaluations the size of typical flow elements will be estimated from spectra for different distances behind the contrail-producing aircraft, in order to follow their temporal development.

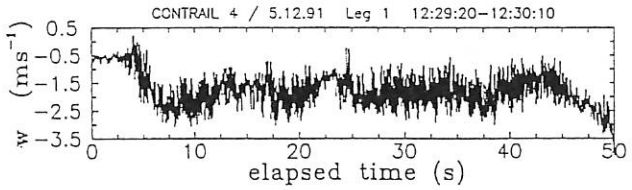

Figure 5. Example record for the vertical wind velocity inside a contrail (Mission Contrail 4, Dec. 5, 1992). The Falcon flew about 2 km behind the leading aircraft, a DC-9.

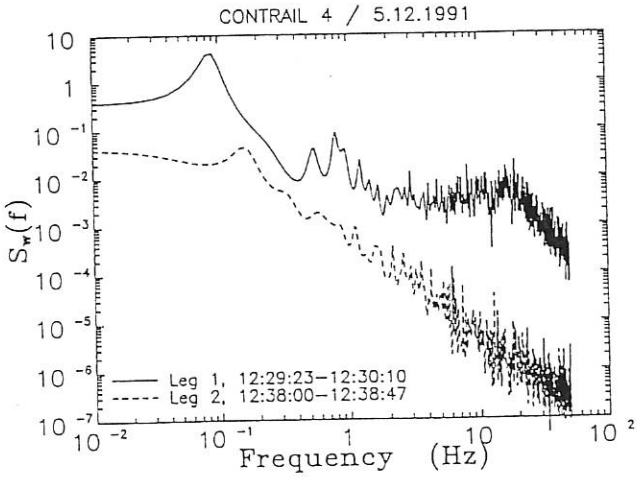

Figure 6. Vertical velocity spectra for flight segments inside the contrail (full line) and in undisturbed air (dashed line). The spectra were estimated using the maximum entropy method.

4. CONCLUSION

In this paper the strategy for inspecting contrails of commercial aircraft by use of the DLR Falcon is outlined, and some examples of measurements are presented. At the moment, these first results look promising, as they confirm the overall strategy and the methods being applied. Although investigations of this kind can be almost case studies on individual contrails, they are considered as an important step to further search into the overall effect of contrails. Therefore this study will be continued, more measurements will be made, and new methods will be applied.

Measurements of chemical species inside and outside of contrails are also part of the program, results will be presented elsewhere.

The effort of Mr. Rox, who worked on the installation of the instruments and did quite a lot of the video handling, was very valuable for the project. The help and the effort of the DLR research flight operations department, especially the work of the pilots, who flew the Falcon under the extremely adverse and exerting conditions, is greatly acknowledged.

5. REFERENCES

Barrodale, I., R.E. Erickson, 1980 : Algorithms for least-squares linear prediction and maximum entropy spectral analysis - Part I: Theory. *Geophysics*, Vol. 45, No. 3, 420-432.

Bögel, W., R. Baumann, 1991 : Test and Calibration of the DLR Falcon Wind Measuring System by Maneuvers. *J. Atmos. Ocean. Technol.*, 8, 5-18.

Burg, J.P., 1967 : Maximum entropy spectral analysis. 37th Ann. Intern. Meeting, Soc. Explor. Geophys., Oklahoma City, Oklahoma.

CIAP, 1975 : Final Report, Department of Transportation, Climatic Assessment Program, DOT-TST-75-51 and ff. (8 vols.).

Ehret, G., C. Kiemle, W. Renger, G. Simmet, 1992 : Airborne Remote Sensing of Tropospheric Water Vapor Using a Near Infrared DIAL System. Submitted to *J. Appl. Opt.*

Fougere, P.F., 1985 : On the accuracy of spectrum analysis of red noise processes using maximum entropy and periodogram methods: Simulation studies and application to geophysical data. *J. Geophys. Res.*, Vol. 90, No. A5, 4355-4366.

Haykin, S., S.Kesler, 1983 : Prediction-error filtering and maximum-entropy spectral estimation. In: S. Haykin (ed.): Nonlinear methods of spectral analysis. 2nd Edition, Springer Verlag, Berlin, 9-72.

Lenschow, D. H., 1984 : Aircraft Measurements in the Boundary Layer. *Probing the Atmospheric Boundary Layer*, D. H. Lenschow, Ed., Amer. Meteor. Soc., 39-55.

Miake-Lye, R.C., M. Martinez-Sanchez, R.C.Brown, C.E. Kolb, 1992 : Plume and Wake Dynamics, Mixing, and Chemistry Behind an HSCT Aircraft. *J. Aircraft*, in press.